# Attempt to Fix the Nucleon-Nucleon Parameters by Examining Nucleon-Nucleus Scattering*

JOSEPH S. CHALMERS AND ALVIN M. SAPERSTEIN
*Department of Physics, Wayne State University, Detroit, Michigan*
(Received 16 September 1966; revised manuscript received 8 December 1966)

The scattering of protons and neutrons from carbon at 142, 210, and 310 MeV is calculated using an optical potential obtained from nucleon-nucleon scattering amplitudes with the impulse, single-scattering, and energy-shell approximations. The integral scattering equation in momentum space is solved numerically using this potential. The present calculation is compared to previous approximate solutions and to the data. An attempt is made to choose among the currently available nucleon-nucleon phase-shift sets.

## I. INTRODUCTION

WATSON[1] has shown that it is possible to express the optical potential for elastic nucleon-nucleus scattering in terms of nucleon-nucleon scattering amplitudes. A persistent hope has been that by using this potential to calculate the differential cross section and polarization for the scattering of nucleons by nuclei, one might be able to make a choice among the various parametrizations of the two-nucleon scattering matrix by comparison with the nucleon-nucleus data. (In the following, we shall refer to nucleon-nucleon scattering by $N$-$N$ and to nucleon-nucleus scattering by $N$-$\mathfrak{N}$.)

Previous studies have employed various approximations in calculating the $N$-$\mathfrak{N}$ scattering observables from the $N$-$N$ amplitudes. One such approximation[2] is the neglect of the variation of the $N$-$N$ transition matrix elements with momentum transfer. This approximation implies that the nuclear potential has the same shape as the nuclear density (see Sec. II) and has the effect of underestimating the range of the $N$-$\mathfrak{N}$ force.[3] Further, as pointed out by Bethe,[2] the imaginary part of the optical potential in momentum space for zero momentum transfer is determined by the $N$-$N$ forward scattering amplitudes, and hence by the $N$-$N$ total cross section. Optical potentials calculated from all phase-shift sets which correctly give the $N$-$N$ total cross section would therefore have nearly the same imaginary parts. This would make any choice among phase-shift sets rather difficult, particularly at 310 MeV, where the central optical potential is primarily imaginary. For this reason, it is necessary to include the momentum-transfer variation of the $N$-$N$ amplitudes; this requires the calculation of $N$-$\mathfrak{N}$ scattering observables at nonforward angles, for which the Born approximation is not even expected to give reasonable predictions for the $N$-$\mathfrak{N}$ polarization. (By the Köhler-Levintov[4] theorem, the polarization is accurately given by the Born approximation for small scattering angles.) Previous efforts in this direction have obtained approximate solutions to the $N$-$\mathfrak{N}$ scattering problem using a WKB[2] or a distorted-wave Born[5] approximation.

In a recent work by McDonald and Hull,[6] the momentum-transfer variation of the $N$-$N$ amplitudes was included in the calculation of the optical potential. This potential was transformed to coordinate space and used in the numerical solution of the radial Schrödinger differential equation. McDonald and Hull then calculated the double-scattering correction to the potential following the formalism of Johnston[7] for the Yale $N$-$N$ phase-shift set. Their work showed that the double-scattering correction significantly affected the $N$-$\mathfrak{N}$ scattering at 150 MeV but was much less important at 300 MeV.

In the present work, the single-scattering potential is calculated in momentum space as it arises naturally from multiple-scattering theory. This potential is then used to solve the Lippmann-Schwinger integral scattering equation numerically by means of matrix inversion. In addition to performing the calculation in momentum space, our procedure differs from that of McDonald and Hull in the means of extrapolation of the potential to large momentum transfer and in the treatment of the Coulomb potential for proton-nuclear scattering. Our aims are also somewhat different.

The objective of this work is twofold: (i) By performing the present calculation with some of the early $N$-$N$ phase-shift sets, we intend to examine the accuracy of the various approximate methods which have been used in obtaining scattering solutions. (ii) By performing the present calculation with the most recent $N$-$N$ phase-shift sets, we will attempt to choose among them on the basis of $N$-$\mathfrak{N}$ data, insofar as this is possible with the single-scattering potential.

In Sec. II we consider the problem of obtaining the $N$-$\mathfrak{N}$ optical potential in momentum space. In Sec. III, the numerical solution of the Lippmann-Schwinger equation is discussed and a somewhat unusual method of treating the Coulomb amplitude is discussed. The

* Work partly supported by National Science Foundation under Contract No. GP5077.
[1] K. M. Watson, Phys. Rev. **105**, 1388 (1957).
[2] H. A. Bethe, Ann. Phys. (N. Y.) **3**, 190 (1958), hereafter referred to as B.
[3] R. Wilson, Phys. Rev. **114**, 260 (1959).
[4] H. S. Köhler, Nucl. Phys. **1**, 433 (1956); I. I. Levintov, Dokl. Akad. Nauk SSSR **107**, 240 (1956) [English transl.: Soviet Phys. —Doklady **1**, 175 (1956)].
[5] A. M. Saperstein and D. Feldman, Nuovo Cimento **14**, 457 (1959), hereafter referred to as SF.
[6] F. A. McDonald and M. H. Hull, Jr., Phys. Rev. **143**, 838 (1966).
[7] R. R. Johnston, Nucl. Phys. **36**, 368 (1962).

present results are compared with previous calculations and with the data in Secs. IV and V.

Since in addition to the single-scattering approximation, we also employ the impulse and $N$-$N$ energy-shell approximations, our final results cannot be unambiguous. Attempts at corrections to these approximations will be made in later work.

## II. THE OPTICAL POTENTIAL

In Watson's theory[1] of multiple scattering, the optical potential for elastic $N$-$\mathfrak{N}$ scattering is expressed, in terms of $N$-$N$ scattering amplitudes, as a sum involving all orders of multiple scattering. The first term in this series can be interpreted as the scattering of the incident nucleon by a single bound in the nucleus. The second term implies successive scatterings of the incident nucleon by two different nucleons in the nucleus and so forth. We will confine ourselves to the first term in this series: the single-scattering approximation. In addition, we use the impulse approximation and, neglecting the binding energy of the struck nucleon and the difference between the $N$-$N$ and $N$-$\mathfrak{N}$ energy shells, use the free $N$-$N$ scattering amplitudes to calculate the optical potential. We will postpone the discussion of these approximations, except to mention that they are expected to improve with increasing energies.

We write the optical potential in momentum space in the form

$$\langle \mathbf{k}' | V | \mathbf{k} \rangle = A \langle \mathbf{k}' | \bar{t} | \mathbf{k} \rangle F(q) , \tag{2.1}$$

where $\mathbf{k}$, $\mathbf{k}'$ are the initial and final momenta of the incident nucleon, respectively, in units of $\hbar$, $\mathbf{q}=\mathbf{k}'-\mathbf{k}$ is the momentum transfer, $\bar{t}$ is the $N$-$N$ transition matrix averaged over spin and isospin states, $F(q)$ is the nuclear form factor, and $A$ is the target mass number. The relation between the $N$-$N$ scattering matrix $t$ and the $N$-$N$ scattering amplitude $f$ is

$$\langle \mathbf{k}' | t | \mathbf{k} \rangle = (-4\pi\hbar^2/m) f(\mathbf{k}',\mathbf{k}) , \tag{2.2}$$

where $m$ is the nucleon mass. Upon averaging over spin and isospin states for a spin-zero target nucleus, we have[5]

$$\bar{f}(\mathbf{k}',\mathbf{k}) = \bar{g}(\mathbf{k}',\mathbf{k}) + \bar{h}(\mathbf{k}',\mathbf{k}) \boldsymbol{\sigma}\cdot\hat{n} , \tag{2.3}$$

where

$$\hat{n} = \mathbf{k}\times\mathbf{k}'/|\mathbf{k}\times\mathbf{k}'| ,$$

so that

$$\langle \mathbf{k}' | V | \mathbf{k} \rangle = -\frac{A 4\pi\hbar^2}{m} [\bar{g}(\mathbf{k}',\mathbf{k}) + \bar{h}(\mathbf{k}',\mathbf{k}) \boldsymbol{\sigma}\cdot\hat{n}] F(q) . \tag{2.4}$$

The identity of the incident and target nucleons is incorporated in the formalism by using the properly symmetrized $N$-$N$ amplitudes.[8]

Since the $N$-$N$ amplitudes are defined only for $q \leq k_L$, where $\hbar k_L$ is the momentum of the incident nucleon in the lab system, the expression (2.4) gives the potential in momentum space only for this limited range of $q$. If we regard the potential in momentum space as a Fourier transform of the coordinate-space potential, then knowledge of the potential in momentum space only for limited $q$ is equivalent to knowing only the gross features of $V(r)$.

In order to solve the scattering equation, however, the potential in momentum space must be known for all momentum transfers. That is, we must extrapolate the potential (2.4) into the region of large $q$ in a way which is physically reasonable and which joins smoothly onto (2.4). There is no point in looking for an exact extrapolation of Eq. (2.4), since the difference between the $N$-$N$ and $N$-$\mathfrak{N}$ energy shells implies that (2.4) itself is an increasingly poor approximation for increasing momentum transfer even in the region for which $g$ and $h$ are known. We expect the small-angle $N$-$\mathfrak{N}$ scattering to be insensitive to the particular method of extrapolation used; the form factor causes the potential to decrease rapidly with increasing $q$, so that the detailed contribution of the large-$q$ region to the small-$q$ region in the Born expansion of the Schrödinger equation should not be very important. Such an assumption should be, and was, tested by using different extrapolation procedures.

The particular procedure we finally used was to assume that the potential in coordinate space is of the usual Fermi spin-orbit form

$$V(r) = V_c(r) + \frac{1}{r}\frac{d}{dr} V_s(r) \boldsymbol{\sigma}\cdot\mathbf{l} , \tag{2.5}$$

where $\hbar\mathbf{l}$ is the relative angular momentum of the nucleon and nucleus. In momentum space, Eq. (2.5) becomes

$$\langle \mathbf{k}' | V | \mathbf{k} \rangle = V_c(q) - i V_s(q) \boldsymbol{\sigma}\cdot(\mathbf{k}\times\mathbf{k}') . \tag{2.6}$$

We adopt the normalization

$$\langle \mathbf{k}' | \mathbf{k} \rangle = (2\pi)^3 \delta(\mathbf{k}'-\mathbf{k}) ,$$

so that

$$V_c(q) = \int e^{-i\mathbf{q}\cdot\mathbf{r}} V_c(\mathbf{r}) d\mathbf{r} ,$$

and similarly for $V_s$. Comparing Eqs. (2.4) and (2.6), we can make the association

$$V_c(q) = -(A 4\pi\hbar^2/m) \bar{g}(q) F(q) , \quad q < k_L ; \tag{2.7a}$$

the extrapolation to $q \geq k_L$ is made by taking

$$V_c(q) = -(A 4\pi\hbar^2/m) \bar{g}(k_L) F(q) , \quad q > k_L . \tag{2.7b}$$

Association of the spin-orbit force with the $N$-$N$ amplitudes is not so straightforward because $\bar{h}$ is of the form

$$\bar{h}(\mathbf{k}',\mathbf{k}) = \tilde{h}(\mathbf{k}',\mathbf{k}) \sin\Theta , \tag{2.8}$$

where $\Theta$ is the elastic scattering angle in the $N$-$N$ center-of-mass (c.m.) system corresponding to the

[8] G. Takeda and K. M. Watson, Phys. Rev. **97**, 1339 (1955).

scattering $\mathbf{k}\rightarrow\mathbf{k}'$ in the $N$-$\mathfrak{N}$ c.m. system; $q=k_L$, where the extrapolation begins, corresponds to backward scattering in the $N$-$N$ system, so that $\sin\Theta$ and $\bar{h}$ vanish. Following Riesenfeld and Watson,[9] we relate the spin-dependent parts of (2.4) and (2.6) for small angle scattering where the $N$-$N$ energy shell difference is small. Using (2.8), we have

$$iV_s(q)k^2\theta\boldsymbol{\sigma}\cdot\hat{n}=(4A\pi\hbar^2/m)\tilde{h}(\mathbf{k}',\mathbf{k})\Theta\boldsymbol{\sigma}\cdot\hat{n}\,, \quad (2.9)$$

where $\theta$ is the scattering angle in the $N$-$\mathfrak{N}$ center of mass system. Since for $\Theta$, $\theta$ both small,

$$\Theta=[2A/(1+A)]\theta\,,$$

we may write

$$V_s(q)=-\frac{i8\pi A^2\hbar^2}{mk^2(1+A)}\tilde{h}(q)F(q)\,, \quad q<k_L. \quad (2.10a)$$

This is exact at small angles and is to be regarded as a reasonable extension to larger angles where the $\bar{h}$ appropriate for Eq. (2.4) is not exactly known since we are off the $N$-$N$ energy shell. In analogy with (2.7), we extrapolate to still larger momentum transfer by taking

$$V_s(q)=-\frac{i8\pi A^2\hbar^2}{mk^2(1+A)}\tilde{h}(k_L)F(q)\,, \quad q>k_L. \quad (2.10b)$$

Equations (2.7b) and (2.10b) give the final form of extrapolating the potential to large $q$ used in this work. However, we have also used other extrapolations. The first consisted simply of setting $V(q)$ equal to zero for $q>k_L$;[6] the second involved treating $\bar{h}$ as a function of $q$ only while taking the central potential as given by (2.7a) and (2.7b). The scattering observables were not greatly affected at angles less than 40° by the method of extrapolation used. Tests were also made with square wells using the extreme "extrapolation": $V_c=V_s=0$ for $q>k_L$; again no major small-angle changes were observed.

### Form Factor

We use the form factor derived from the modified Gaussian density distribution used by Fregeau[10] to fit electron-carbon scattering data. This distribution has the form

$$\rho(r)=\rho_0[1+w(r/a)^2]e^{-(r/a)^2}\,,$$

with $a=1.635$ F and $w=\frac{4}{3}$ for carbon. The resultant form factor is

$$F(q)=[1-(qa)^2/9]e^{-(qa)^2/4}.$$

### Charged Particles

The potential (2.4) is interpreted to be the potential between a neutron and the nucleus. For protons, we add to this potential an extended charge Coulomb potential with a charge distribution identical to the nuclear distribution. This potential in momentum space is

$$V_{\mathrm{Coul}}(q)=4\pi Ze^2F(q)/q^2. \quad (2.11)$$

This procedure assures that for a target nucleus with equal numbers of protons and neutrons, the potential for an incident proton and neutron differ only by the usual, additive, Coulomb potential. Inclusion of the Coulomb contribution to the $N$-$N$ amplitudes as done in Ref. 5 leads to a mixing of the Coulomb and nuclear potentials, as well as a complex Coulomb potential. Since the Coulomb potential does not satisfy the condition that the range of the force be less than the mean spacing of the target nucleons, the impulse approximation cannot be applied to the complete $N$-$N$ amplitude. In the work of Kerman *et al.*,[11] the scattering equation is solved using the potential (2.4) multiplied by $(A-1)/A$. If one does this, however, it is unclear how the Coulomb potential is to be included. Johansson *et al.*[12] accomplish this by adding to the potential of KMT the Coulomb potential of (2.11) also multiplied by $(A-1)/A$. This procedure retains the proper relative magnitude of the nuclear and Coulomb potentials, but it is difficult to see any further grounds for this procedure. For this reason, we have followed the method of Watson.

### Errors from Approximations

The error due to the impulse approximation involves the difference between the $N$-$N$ scattering matrix with one of the nucleons bound in the nucleus ($t$), and with both nucleons free ($t_0$). It is shown in Ref. 11 that if

$$t=t_0+\Delta t\,,$$

then

$$\Delta t/t\sim\langle K\rangle/E\,,$$

where $\langle K\rangle$ is the average kinetic energy of a nuclear particle, and $E$ is the incident energy. Since $\langle K\rangle\sim18$ MeV,[13] this correction ranges between 12% and 6% for $E$ of 150 and 300 MeV, respectively.

The double-scattering correction involves excitation of the nucleus by the collision of the incident particle with one of the target nucleons followed by de-excitation of the nucleus in the collision with a second target nucleon. This correction requires knowledge of the two-body correlation function of the target nucleons and leads to a correction to the central potential of the order[11]

$$\Delta V_c(r=0)\sim iV_c^2kR_c/2E\,,$$

[9] W. B. Riesenfeld and K. M. Watson, Phys. Rev. **102**, 1157 (1956).
[10] J. H. Fregeau, Phys. Rev. **104**, 225 (1956).
[11] A. K. Kerman, H. McManus, and R. M. Thaler, Ann. Phys. (N. Y.) 8, 551 (1959), hereafter referred to as KMT.
[12] A. Johansson, U. Svanberg, and P. E. Hodgson, Arkiv Fysik **19**, 541 (1961).
[13] See, for example, E. Segrè, *Nuclei and Particles* (W. A. Benjamin, Inc., New York, 1964), p. 472.

where $R_c$ is the correlation length, which we take to be $\sim$0.5 F. At 150 MeV, the real and imaginary parts of $V_c$ are roughly the same and the correction increases the real part by $\sim$25%. At 300 MeV, $V_c$ is almost entirely imaginary and the correction is also imaginary and about 7% of $V_c$.

Combining the errors from both approximations, the error in the potential could be as much as 37% at 150 MeV or 13% at 300 MeV. The corresponding error in the cross section would be 90% at 150 MeV and 28% at 300 MeV. The error in the polarization would be roughly half that of the cross section. These estimates can be obtained by using the Born approximation and the fact that the corrections are primarily to the central potential.

## III. THE SCATTERING EQUATION

We use the potential described in Sec. II to solve the scattering equation,

$$\langle \mathbf{k}'|T|\mathbf{k}_0\rangle = \langle \mathbf{k}'|U|\mathbf{k}_0\rangle - \frac{1}{(2\pi)^3}\int \frac{\langle \mathbf{k}'|U|\mathbf{K}\rangle\langle \mathbf{K}|T|\mathbf{k}_0\rangle d\mathbf{K}}{K^2-k_0^2-i\epsilon}, \quad (3.1)$$

where $\mathbf{k}_0$, $\mathbf{k}'$ are, respectively, the initial and final relative wave vectors in the $N$-$\mathfrak{N}$ c.m. system, $U=2\mu V/\hbar^2$, $\mu$ being the reduced mass in the $N$-$\mathfrak{N}$ system, and $T$ is the $N$-$\mathfrak{N}$ scattering matrix. For the scattering of spin-$\frac{1}{2}$ nucleons by spin-zero nuclei, $T$ and $U$ are $2\times2$ matrices in spin space.

In order to find the partial-wave decomposition of (3.1), we expand the incident plane wave with spin component $m_s$ parallel to $\mathbf{k}$ as

$$|\mathbf{k},m_s\rangle = 4\pi\sum_{l,m} i^l j_l(kr) Y_l^{m*}(\hat{k}) \sum_j C_{l,1/2,m,m_s}^{j,m_j=m+m_s} \times \mathcal{Y}_{l,1/2}^{j,m_j}(\hat{r}), \quad (3.2)$$

where the sum over $j$ contains two terms for $j=|l-\frac{1}{2}|$ and $l+\frac{1}{2}$, $j_l(x)$ is the regular spherical Bessel function, $Y_l^m(\Omega)$ is the usual spherical harmonic, $C_{l,1/2,m,m_s}^{j,m_j}$ is the Clebsch-Gordan coefficient, $\mathcal{Y}_{l,1/2}^{j,m_j}(\hat{r})$ is the eigenfunction of $l^2$, $\sigma^2$, $j^2$, and $j_z$, where $\mathbf{j}$ is the total angular momentum in units of $\hbar$

$$\mathbf{j}=\mathbf{l}+\tfrac{1}{2}\boldsymbol{\sigma}.$$

The expansion for $|\psi(\mathbf{k},m_s)\rangle$, the state evolving from $|\mathbf{k},m_s\rangle$ under the potential $V$, is, similarly,

$$|\psi(\mathbf{k},m_s)\rangle = 4\pi\sum_{l,m} i^l Y_l^{m*}(\hat{k}) \sum_j C_{l,1/2,m,m_s}^{j,m_j} \psi_l^j(kr) \times \mathcal{Y}_{l,1/2}^{j,m_j}(\hat{r}). \quad (3.3)$$

The operator $T$ is defined as usual by

$$\langle m_s',\mathbf{k}'|T|\mathbf{k},m_s\rangle \equiv \langle m_s',\mathbf{k}'|U|\psi(\mathbf{k},m_s)\rangle. \quad (3.4)$$

Using (3.2), the spin-space matrix elements of $U$ are given by

$$\langle +,\mathbf{k}'|U|\mathbf{k},+\rangle = 4\pi\sum_l P_l(\hat{k}'\cdot\hat{k}) \times[(l+1)U_l^+(k',k)+lU_l^-(k',k)],$$
$$\langle -,\mathbf{k}'|U|\mathbf{k},+\rangle = -4\pi e^{i\phi}\sum_l P_l^1(\hat{k}'\cdot\hat{k}) \times[U_l^+(k',k)-U_l^-(k',k)], \quad (3.5a)$$
$$\langle -|U|-\rangle = \langle +|U|+\rangle,$$
$$\langle +|U|-\rangle = -e^{-2i\phi}\langle -|U|+\rangle,$$

where $|\pm\rangle \equiv |m_s=\pm\tfrac{1}{2}\rangle$. The partial-wave expansions for $\langle T\rangle$ are obtained from (3.5a) by replacing $U$ by $T$ everywhere. If $U(r)$ is of the form

$$U(r)=U_c(r)+U_s(r)\boldsymbol{\sigma}\cdot\mathbf{l},$$

then the $U_l^{(\pm)}$ are defined by

$$U_l^{(\pm)}(k',k) = \int_0^\infty j_l(k'r) j_l(kr) \times\left[U_c(r)+U_s(r)\begin{pmatrix} l \\ -l-1\end{pmatrix}\right] r^2 dr, \quad (3.5b)$$

while for $T_l^{(\pm)}$ we have

$$T_l^{(\pm)}(k',k) = \int_0^\infty j_l(k'r)\psi_l^{j=l\pm1/2}(kr) \times\left[U_c(r)+U_s(r)\begin{pmatrix} l \\ -l-1\end{pmatrix}\right] r^2 dr. \quad (3.5c)$$

If we now combine the partial-wave decompositions (3.5) with the scattering equation (3.1), we obtain the uncoupled integral equations

$$T_l^{(\pm)}(k',k_0) = U_l^{(\pm)}(k',k_0) - \frac{2}{\pi}\int_0^\infty \frac{U_l^{(\pm)}(k',K)T_l^{(\pm)}(K,k_0)K^2dK}{K^2-k_0^2-i\epsilon}. \quad (3.6)$$

### Numerical Calculations

The numerical solution of the scattering problem consists of extracting the expansion coefficients from Eq. (3.5) and using these to solve the scattering equation (3.6).

The expansion coefficients in (3.5) are obtained by means of the orthogonality of the Legendre polynomials on the interval $-1$ to 1. The integrations involved are performed numerically by 24-point Gaussian quadrature. This procedure has been tested using a square-well potential, which is highly oscillatory in momentum

space. The expansion coefficients in this case were given to no less than six-place accuracy. The $U_l^{(\pm)}$ were obtained for $k$, $k'$ pairs chosen for the numerical solution of equations (3.6).

The integral equation (3.6) for $T_l^{(\pm)}$ is solved by representing the principal part of the integral over $K$ as a sum by an $n$-point numerical quadrature. The real and imaginary parts of Eq. (3.6) then form a set of $2(n+1)$ coupled linear equations; the $T_l^{(\pm)}(k,k_0)$ are then obtained by matrix inversion. We retain the real and imaginary parts of

$$T_l^{(\pm)}(k_0,k_0)=-(e^{2i\delta_l^{\pm}}-1)/2ik_0,$$

where $\delta_l^{\pm}$ is the complex $N$-$\mathfrak{N}$ phase shift for $j=l\pm\frac{1}{2}$.

We have found that the greatest accuracy is obtained by performing a Gaussian quadrature separately in each of the two intervals above and below the singularity at $k_0$. As might be expected, accuracy is improved by increasing the number of quadrature points in the evaluation of the principal part integral. However, because of the limitations of computer size (an IBM 7074), we were able to use only ten-point quadrature in each half of the integral.

In testing the numerical procedure, we have used a square well of depth and range comparable to the nuclear potential. On this basis, we believe that the phase shifts which we calculate are accurate to four places, which should be ample since variation in the third place is barely noticeable in plotting the scattering observables.

### Treatment of the Coulomb Potential

The form of the scattering equation (3.1) is strictly valid only for a short-range potential and not for the long-range Coulomb potential. However, it is found that when the numerical-solution procedure described above is carried out for a point-charge potential, the phase shifts obtained differ from the usual Coulomb phase shifts by a constant independent of $l$. That is,

$$\sigma_l^{\text{calc}}=\sigma_l+\alpha, \tag{3.7}$$

where

$$\sigma_l=\arg\Gamma(l+1+i\eta), \tag{3.8}$$
$$\eta=Ze^2/\hbar v,$$

and $v$ is the relative velocity of the incident and target particles. It is further found that $\alpha$ is proportional to $\eta$. This can be roughly understood in the following way.

The Coulomb potential in momentum space is singular at $q=0$. The integrals for determining the expansion coefficients as in (3.5) do not exist. However, when the integrals are performed numerically, a finite answer is, of course, obtained. This is equivalent to $V(q=0)$ being finite, which in turn implies that $V(r)$ has a finite range. Now, regardless of how the finite range appears in $V(r)$, it can be seen that

$$V(q=0)\sim a^2, \tag{3.9}$$

where $a$ is an appropriate range parameter. On the other hand, examining the numerical integration leading to the expansion coefficients of (3.5), we see that for the Coulomb potential,

$$V(q)\sim\frac{1}{q^2}=\frac{1}{2k_0^2(1-x)},$$

where $x$ is the cosine of the scattering angle, so that

$$V_l(k_0,k_0)\sim\frac{1}{k_0^2}\int_{-1}^{1}\frac{P_l(x)dx}{1-x}=C_l/k_0^2,$$

where $C_l$ depends on the details of the quadrature procedure. Therefore, using this result in (3.5), we see that the numerical quadrature imposes

$$V(q=0)\sim 1/k_0^2. \tag{3.10}$$

Comparing (9) and (10) we see that

$$a\sim 1/k_0. \tag{3.11}$$

We now consider the simplest way in which the range of the Coulomb potential can be made finite, namely, a Gordon-sphere cutoff in which

$$\begin{aligned} V(r)&=Ze^2/r, && r<a \\ &=0, && r>a. \end{aligned} \tag{3.12}$$

Assume $a$ is large enough so that the radial wave function

$$\begin{aligned} u_l(r)&\sim\sin[kr-\eta\ln(2kr)-\tfrac{1}{2}l\pi+\sigma_l], && r<a \\ &\sim\sin(kr-\tfrac{1}{2}l\pi+\sigma_l^{\text{calc}}), && r>a. \end{aligned} \tag{3.13}$$

Matching the radial functions (3.13) at $r=a$, we find

$$\sigma_l^{\text{calc}}=\sigma_l-\eta\ln(2ka),$$

and using (3.11)

$$\sigma_l^{\text{calc}}=\sigma_l-C\eta, \tag{3.14}$$

which obviously is of the desired form (3.7). The numerical projection of the partial-wave components of the Coulomb potential is then equivalent to imposing a finite range on the potential, which in turn enables us to use the scattering equation (3.1) for the scattering of charged particles.

Finally, the scattering amplitude is obtained by solving the scattering equation (3.6), including the Coulomb part (2.11), in the potential, for all $l$ up to some $l_{\max}$ determined by the range of the nuclear force and the energy. We took $l_{\max}=17$ for all energies considered. For higher $l$, the nuclear part of the phase shift is negligible and the Coulomb part of the phase shift is adequately given by the point-charge phase shift. The

non-spin-flip amplitude is then given by

$$g(\theta)=\frac{1}{2ik_0}\sum_{l=0}^{l_{\max}}[(l+1)(e^{2i\delta_l^+}-1)+l(e^{2i\delta_l^-}-1)]P_l(\theta)$$
$$+\frac{1}{2ik_0}\sum_{l=l_{\max}+1}^{\infty}(2l+1)(e^{2i\sigma_l^{\rm calc}}-1)P_l(\theta),$$
$$=\frac{1}{2ik_0}\sum_{l=0}^{l_{\max}}[(l+1)e^{2i\delta_l^+}+le^{2i\delta_l^-}-(2l+1)e^{2i\sigma_l^{\rm calc}}]$$
$$\times P_l(\theta)+e^{2i\alpha}g_{\rm Coul}(\theta),$$

where $\delta_l$ is the phase shift obtained from (3.6) with the nuclear-plus-extended-charge Coulomb potential $\sigma_l^{\rm calc}$ is given by (3.7) and $g_{\rm Coul}(\theta)$ is the usual point-charge Coulomb amplitude.

$$g_{\rm Coul}(\theta)=-[\eta/2k_0\sin^2(\tfrac{1}{2}\theta)]e^{2i[\sigma_0-\eta\ln(\sin\frac{1}{2}\theta)]}.$$

## IV. COMPARISONS WITH PREVIOUS APPROXIMATIONS

The purpose of this section is to investigate the accuracy of the various approximate solutions to the scattering of protons from carbon by the single-scattering potential. Although some of the phase-shift sets used in these early calculations are no longer considered to be among the best representatives of $N$-$N$ data, we perform the present calculation using these sets in order to compare with the previously reported approximate solutions which have used these same phase-shift sets.

*310 MeV.* Approximate calculations of the scattering of protons from carbon at 310 MeV have been carried out by Bethe,[2] Cromer,[14] and Kerman *et al.*[11] using the WKB approximation, and by Saperstein and Feldman[5] using the distorted-wave Born (DWB) approximation. B, C, and SF performed the calculation using the Stapp[15] No. 1 phase-shift set together with the complementary Gammel-Thaler[16] singlet set; and we have used this set in the present calculation in order to compare with these calculations. The variation of the $N$-$N$ amplitudes was ignored in B and was included to first order in $q^2$ in C. SF and the present calculation include this variation to all orders in $q^2$. Since inclusion of the variation of the $N$-$N$ amplitudes implies a larger effective radius of the potential, we would expect the diffraction pattern of C to be shifted to smaller angles than that of B. The small-angle cross section of C, however, is identical to that of B. In Fig. 1, it is seen that the DWB cross section agrees very well with the present calculation at small angles. Furthermore, the DWB cross section and the present calculation are shifted to smaller angles than that of B and C, indicating a still larger effective radius than in C.

In Fig. 2, it is seen that all the calculated polarizations agree fairly well, with B and the present calculation virtually identical at small angles. Since the polarization depends on the phase as well as the magnitude of the $N$-$\mathfrak{N}$ amplitudes, it is understandable that calculations giving exactly similar cross sections could give less precise agreement in the polarization, as in Figs. 1 and 2.

At 310 MeV, we can conclude that all the calculations are reliable for both cross section and polarization, with the DWB cross section somewhat better at small angles. The DWB polarization agrees qualitatively with the present calculation for a large angular range. In particular, we note the agreement in the positions of the polarization maxima and minima given by the two calculations (Fig. 2).

*135 MeV.* The scattering of protons from carbon at 135 MeV was calculated by SF, again using the DWB approximation. To compare with SF, we have performed the present calculation using the Signell-Marshak[17] phase-shift set. In Fig. 3, we can see the qualitative agreement of the calculations. As at 310 MeV, the exact cross section falls below the DWB cross section at large angles, indicating insufficient absorption in the latter. In the small-angle range, the DWB calculation overemphasizes the Coulomb interference.

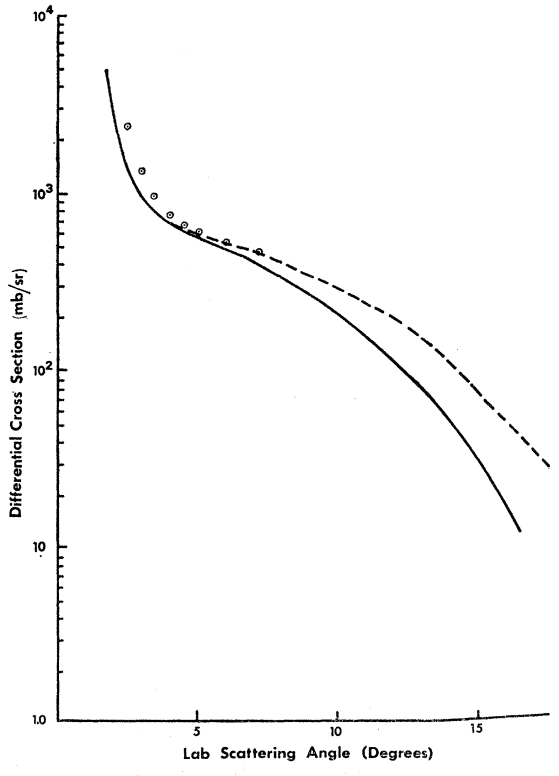


FIG. 1. Calculated $p$-carbon differential cross section in millibarns at 310 MeV. Solid curve is the present calculation, dashed curve is DWB (SF) and open circles are WKB (B).

[14] A. H. Cromer, Phys. Rev. **113**, 1607 (1959), hereafter referred to as C.
[15] H. P. Stapp, T. J. Ypsilantis, and N. Metropolis, Phys. Rev. **105**, 302 (1957), hereafter referred to as SYM.
[16] See Ref. 2 for details.
[17] P. S. Signell and R. E. Marshak, Phys. Rev. **109**, 1229 (1958).

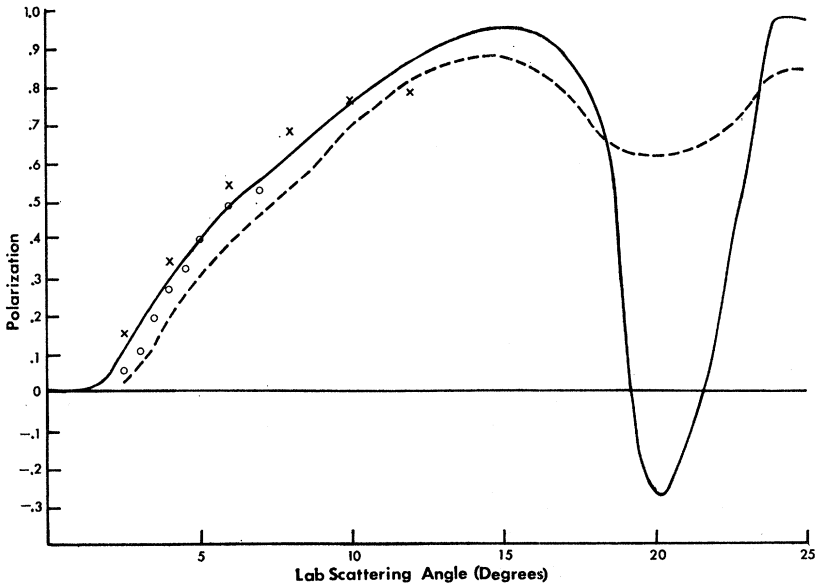


FIG. 2. Calculated $p$-carbon polarization at 310 MeV. Solid curve is the present calculation, dashed curve is DWB (SF), crosses for WKB (C), and open circles for WKB (B).

This is undoubtedly due to the different methods of treating the Coulomb amplitudes used in the two calculations. This overemphasis of the Coulomb interference does not occur at 310 MeV in the DWB calculation because at 310 MeV the nuclear amplitude is nearly all imaginary, while the Coulomb amplitude is almost completely real; hence, there will be small interference.

In Fig. 4, the polarizations agree well to 5°, after which the DWB values lie below the exact by about 20%. There is qualitative agreement, however, to ~20°.

In comparing the approximate calculations with the present solution of the Lippmann-Schwinger equation at various energies, we conclude that there is little energy dependence in the relation between them. Furthermore, both the WKB and DWB approximations give adequate quantitative representations of the small-angle cross section and polarization. An interesting point, to be discussed later, is that the DWB gives qualitative agreement with the experimental polarization over a large range of angles for the energies used here.

As described in Sec. I, McDonald and Hull[6] perform a calculation very similar to the present one using the Yale[18] phase-shift set. Our calculation, with a single-scattering potential for $p$-carbon scattering at 142 and 310 MeV using the Yale set, appears to give results which are identical to the corresponding calculation of McDonald and Hull (which they label $V^{(1)}$). Furthermore, the double-scattering correction of McDonald and Hull changes the observables by amounts which are *well within the estimates given in Sec. II.*

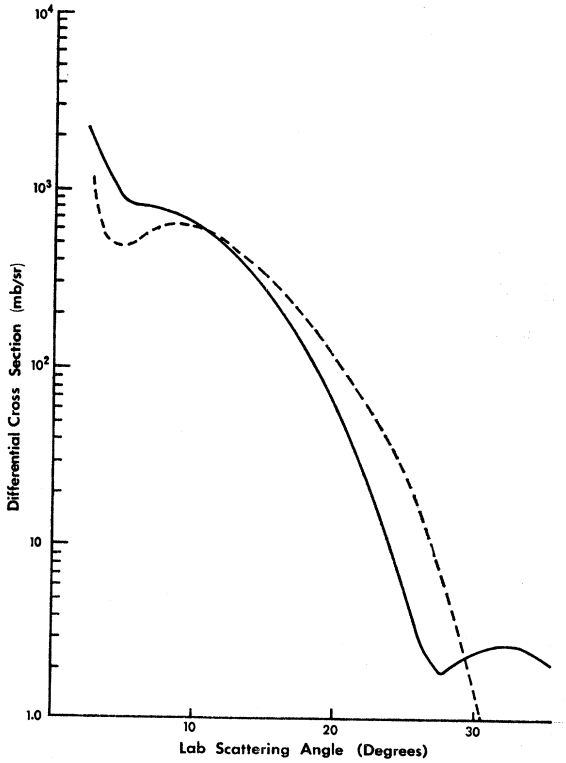


FIG. 3. Calculated $p$-carbon differential cross section in millibarns at 142 MeV. Solid curve is present calculation and dashed curve is DWB (SF).

[18] G. Breit, M. H. Hull, Jr., K. E. Lassila, K. D. Pyatt, Jr., and H. M. Ruppel, Phys. Rev. 128, 826 (1962); M. H. Hull, Jr., K. E. Lassila, M. H. Ruppel, F. A. McDonald, and G. Breit, *ibid.* 128, 830 (1962). Sets YLAM and YLAN3M were used.

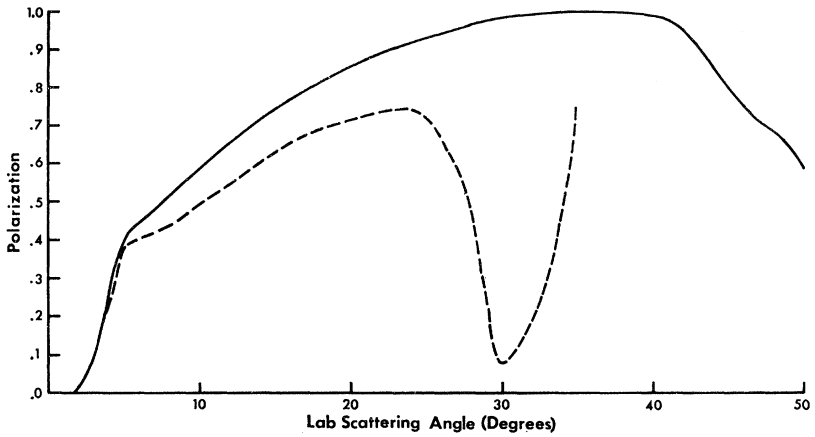


FIG. 4. Calculated $p$-carbon polarization at 142 MeV. Solid curve is present calculation and dashed curve is DWB(SF).

## V. COMPARISON WITH DATA

*p-Carbon.* At 142 MeV, we have tested the Yale,[18] Dubna,[19] Livermore,[20] Harwell[21] and Signell-Marshak phase-shift sets. The first four sets are among the most recent and their similarity has been interpreted as evidence that the $N$-$N$ scattering matrix has nearly been determined at this energy. We use the data of Dickson and Salter,[22] Taylor and Wood,[23] and Steinberg, Palmieri, and Cormack.[24] The polarization data[22,24] has been adjusted downward following the results of Jarvis and Rose.[25]

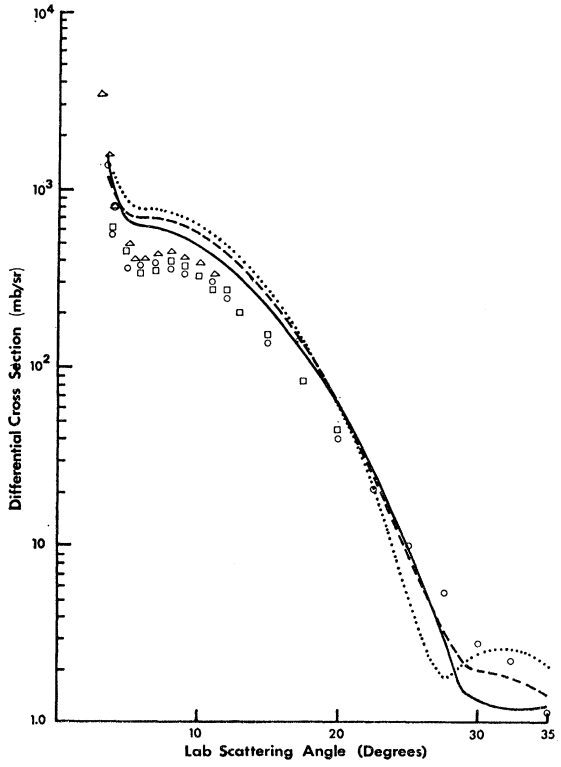


FIG. 5. Calculated $p$-carbon differential cross section versus data, in millibarns at 142 MeV. Solid curve is for Yale set, dashed curve is for Livermore set and dotted curve is for Signell-Marshak set. Data marked by circles from DS (Ref. 22), by squares from TW (Ref. 23); and by triangles from SPC (Ref. 24). For this and succeeding figures, the absence of error bars implies the stated errors are smaller than the data symbol.

At 210 MeV, the Yale and Livermore sets were tested against the polarization data of Hafner[26] and the cross section data of Thwaites[27]; and at 310 MeV the Yale, Livermore, and SYM No. 1-GT sets were tested against the data of Chamberlain *et al.*[28]

*Differential Cross Section: 142 MeV.* We plot in Fig. 5 the cross section calculated from the optical potential obtained from the Yale, Livermore, and Signell-Marshak phase-shift sets. The plots for the Dubna and Harwell sets lie between the Yale and Livermore plots at small angles. As can be seen from Fig. 5, all the calculated cross sections are high by about 50% at the Coulomb-interference region. The plots then fall below the data as the diffraction minimum is approached. This behavior is indicative that multiple-scattering effects are fairly important at this energy.

*210 MeV.* We plot in Fig. 6 the cross section calculated using the Yale and Livermore phase-shift sets. Again, both plots are somewhat high at small angles, although much less so than at 142 MeV. The plots then fall below the data as the diffraction minimum is approached.

*310 MeV.* In Fig. 7, we plot the cross section calculated using the Yale and Livermore sets. The plot for the SYM No. 1-GT set lies very close to the Yale plot. As can be seen from Fig. 7, the calculated plots

[19] Yu M. Kazarinov, V. S. Kiselev, and I. N. Silin, Zh. Eksperim. i Teor. Fiz. **45**, 637 (1963) [English transl.: Soviet Phys.—JETP **18**, 437 (1964)].
[20] M. H. MacGregor and R. A. Arndt, Phys. Rev. **139**, B362 (1965).
[21] J. K. Perring, Nucl. Phys. **42**, 306 (1963).
[22] J. M. Dickson and D. C. Salter, Nuovo Cimento **6**, 235 (1957).
[23] A. E. Taylor and E. Wood, Nucl. Phys. **25**, 642 (1961).
[24] D. Steinberg, J. N. Palmieri, and A. M. Cormack, Nucl. Phys. **56**, 46 (1964).
[25] O. N. Jarvis and B. Rose, Phys. Letters **15**, 271 (1965).
[26] E. M. Hafner, Phys. Rev. **111**, 297 (1958).
[27] T. T. Thwaites, Ann. Phys. (N. Y.) **12**, 56 (1961).
[28] O. Chamberlain, E. Segrè, R. D. Tripp, C. Wiegand, and T. Ypsilantis, Phys. Rev. **102**, 1659 (1956).

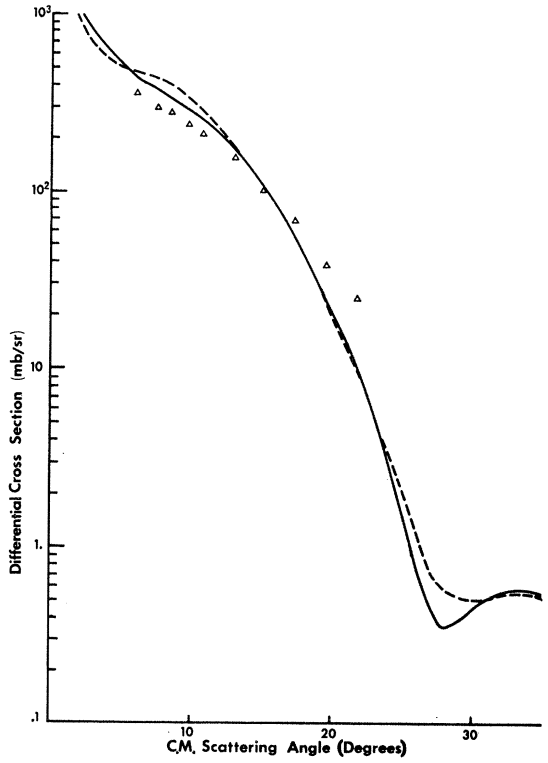


FIG. 6. Calculated $p$-carbon differential cross section versus data in millibarns at 210 MeV. Solid curve is for Yale set and dashed curve is for Livermore set. Triangles for data from Thwaites (Ref. 27).

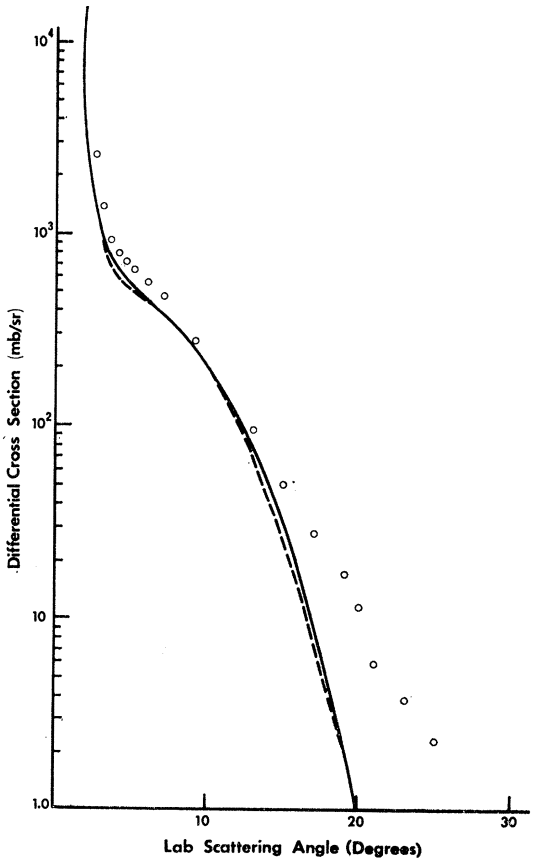


FIG. 7. Calculated $p$-carbon differential cross section versus data, in millibarns at 310 MeV. Solid curve is for Yale set and dashed curve is for Livermore set. Circles for data from Chamberlain *et al.* (Ref. 28).

are low by a very small amount at small angles, and become progressively lower as the diffraction minimum is approached.

Figures 5–7 show the qualitative improvement of the small-angle cross section fits with increasing energy. This would seem to indicate that the importance of the corrections to the single-scattering, impulse, and $N$-$N$ energy-shell approximations decreases with increasing energy.

*Polarization.* As can be seen from Figs. 8–10, quantitative agreement with the data is restricted to small angles. As with the cross section, the qualitative agreement of the fits with the data improves with increasing energy, again indicating decreasing importance of the corrections with increasing energy. It is interesting to see in Fig. 8 that the Signell-Marshak polarization lies closest to the data at 142 MeV.

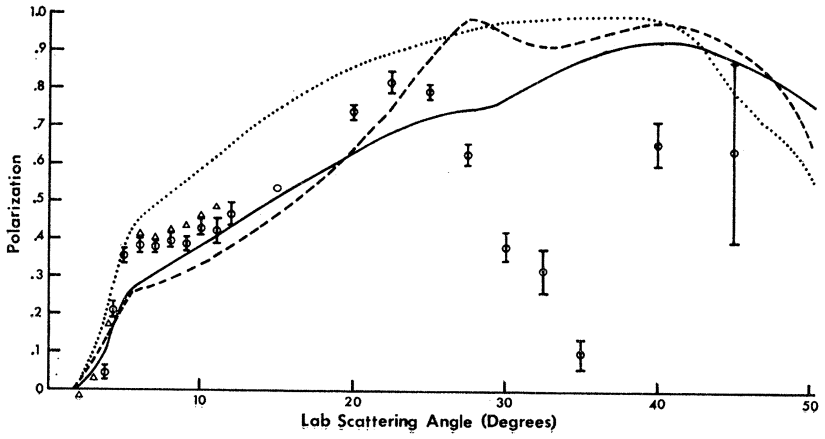


FIG. 8. Calculated $p$-carbon polarization versus data at 142 MeV. Solid curve is for Yale set, dashed curve is for Livermore set, and dotted curve is for Signell-Marshak set. Data marked by circles from DS (Ref. 22); and by triangles from SPC (Ref. 24). Data are adjusted according to Jarvis and Rose (Ref. 25).

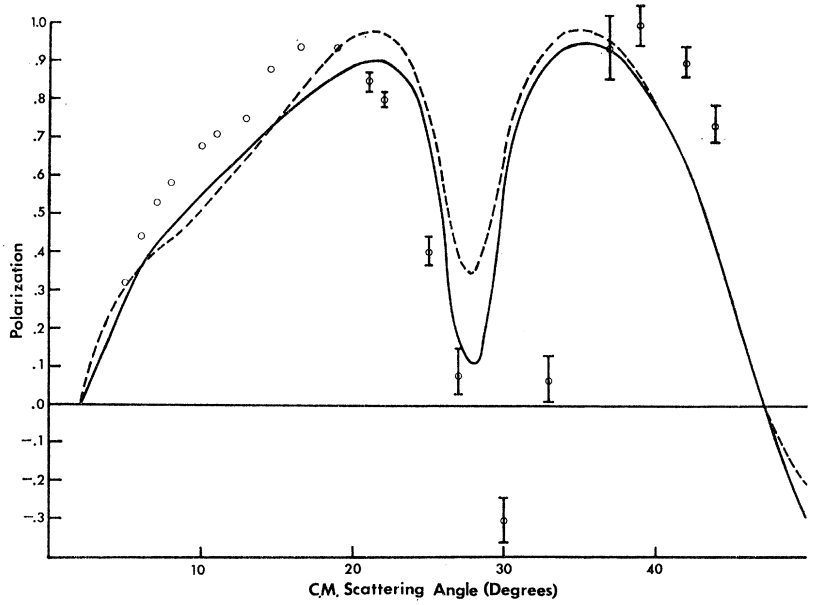


FIG. 9. Calculated $p$-carbon polarization versus data at 210 MeV. Solid curve is for Yale set and dashed curve is for Livermore set. Circles are for data from Hafner (Ref. 26).

A further point to be noted is that the calculated polarizations show pronounced minima at the positions of the diffraction minima at 210 and 310 MeV, but only a shallow minimum at 142 MeV (Figs. 8–10). The DWB polarization at 142 MeV does show a pronounced dip at the differential minimum. A calculation by Johansson *et al.*[12] at 180 MeV also shows a substantial dip. In view of the location of these dips at the expected positions of the diffraction minima, it seems certain that they are due to nuclear size effects. A possible explanation of the absence of the polarization minima from our calculation at 142 MeV can be found in the observation by Kerman *et al.*[11] that the real and imaginary parts of the spin-orbit force have markedly different effective radii at this energy, while the real and imaginary parts of the central potential have nearly the same radii. If the $N$-$\mathfrak{N}$ amplitudes show the same gross features as the potential, the real and imaginary parts of the spin-flip amplitude would have zeroes at markedly different momentum transfers, tending to wash out a sharp minimum. The existence of a sharp minimum in the data at this energy and its qualitative reproduction by the DWB approximation (Fig. 4) is thus a puzzle. It might be viewed as a result of double scattering. Because of the diffraction minimum, very few nucleons of either spin direction are scattered into this region of momentum transfer by the single-scattering potential. If double-scattering puts roughly equal amounts of spin-up and spin-down nucleons into this region, it would diminish the relative difference between the two spin-state populations at this scattering angle and thus produce a smaller polarization. The fact that the DWB approximation, which shows too little absorption at these angles, i.e., scatters extra nucleons into this range much like multiple scattering, also shows the polarization dip might be construed as additional evidence for this view.

*Discrimination Among Phase Shift Sets.* At 142 MeV,

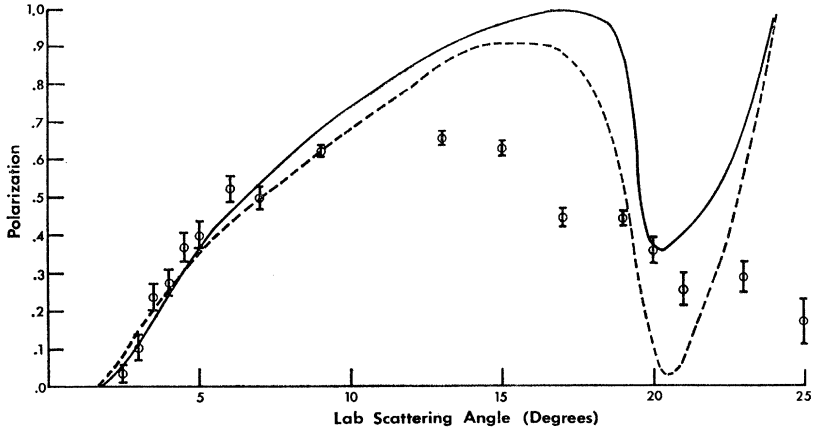


FIG. 10. Calculated $p$-carbon polarization versus data at 310 MeV. Solid curve is for Yale set and dashed curve is for Livermore set. Circles are for data from Chamberlain *et al.* (Ref. 28).

the corrections to the impulse and single-scattering approximations are expected to be considerable, and this is reflected in the fits to the cross section and polarization as can be seen in Figs. 5 and 8. Although the Yale fit lies closest to the data, we believe that a firm choice cannot be made at this energy until the corrections are considered. It is interesting, though probably without significance, that the Signell-Marshak polarization fits the data better than any of the other sets tested.

At 210 MeV, in Fig. 6, the Livermore small-angle cross section is in error by $\sim 50\%$, while for the Yale set the error is $\sim 20\%$. The error due to the impulse and single-scattering approximations, estimated in the manner described in Sec. II, is $\sim 40\%$. The polarization fits, as seen in Fig. 9, are too close to permit any choice.

At 310 MeV, in Fig. 7, the Livermore small-angle cross section is in error by $\sim 35\%$. Since this lies outside the range of the maximum expected error at this energy (see Sec. II), we believe that the Yale fit is favored at this energy. It might be thought that the Livermore polarization is superior, inasmuch as it passes through the 9° data point, which the Yale fit does not. However, the difference between the two predictions is comparable with the uncertainty in the calculation. Moreover, Batty[29] has questioned the compatibility of the normalization of the large- and small-angle data, with the large-angle data beginning at 9°.

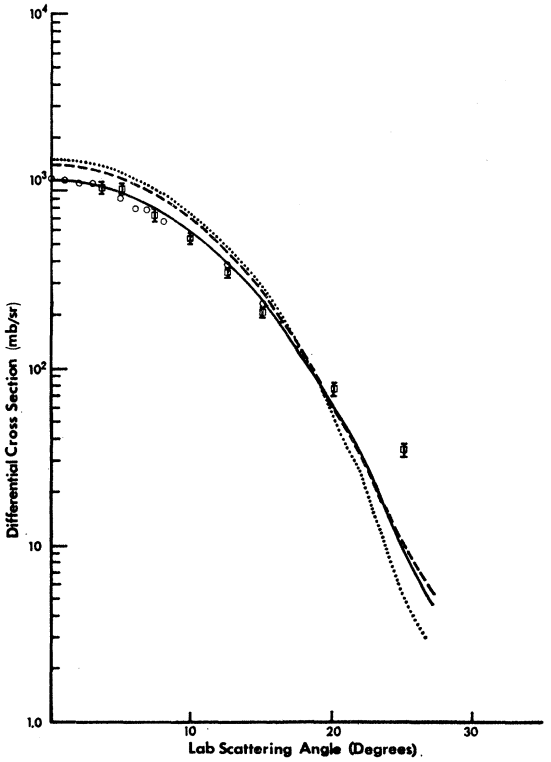


FIG. 11. Calculated $n$-carbon differential cross section versus data in millibarns at 142 MeV. Solid curve is for Yale set, dashed curve is for Livermore set, and dotted curve is for Signell-Marshak set. Circles are for data from VVW (Ref. 31); squares are for data from Harding (Ref. 30).

[29] C. J. Batty, Nucl. Phys. **23**, 562 (1962).

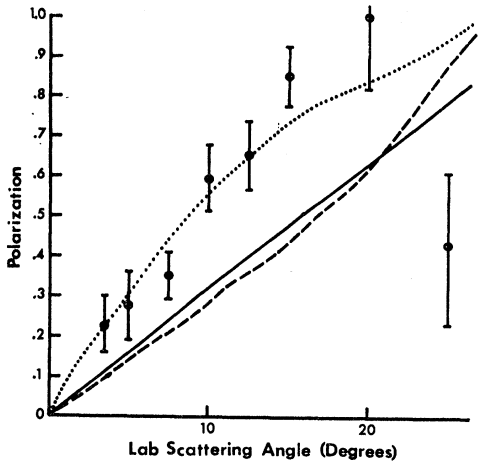


FIG. 12. Calculated $n$-carbon polarization versus data at 142 MeV. Solid curve is for Yale set, dashed curve is for Livermore set, and dotted curve is for Signell-Marshak set. Circles are for data from Harding (Ref. 30).

We conclude that this calculation seems to favor slightly the Yale set at 210 and 310 MeV, and possibly at 142 MeV as well.

*n-Carbon.* In order to strengthen the conclusions drawn from the proton-carbon fits at 142 MeV, we have calculated the neutron-carbon scattering using the Yale, Livermore and Signell-Marshak phase-shift sets. We use the data of Harding[30] and of Van Zyl, Voss, and Wilson.[31] In Fig. 11, it is seen that all the calculated cross sections agree fairly well with the data, with the Yale cross section, apparently the best, passing through the data out to 20°. The small-angle Livermore cross section is high by about 20%, well within the uncertainties of this calculation. In Fig. 12, the Yale and Livermore polarizations are about 50% below the data and can both be considered "fits" within the scope of this work. Again the Signell-Marshak set gives a very good fit to the polarization data. We thus cannot use the neutron-carbon fits to make a definitive choice among these phase shift sets. The neutron-carbon fits, however, do lend further weight to the Yale set.

## VI. CONCLUSION

From the comparisons made in Sec. IV, we can say that the WKB and DWB approximations are fairly reliable at small angles and the DWB approximation exhibits the qualitative features of the present calculation to rather large angles.

The improvement of the fits with increasing energy seen in Sec. V indicates that the impulse, single-scattering, and energy-shell approximations become more accurate with increasing energy, as would be expected.

[30] R. S. Harding, Phys. Rev. **111**, 1164 (1958).

[31] C. P. VanZyl, R. G. P. Voss, and R. Wilson, Phil. Mag. **1**, 1003 (1956), hereafter referred to as VVW.

Furthermore, it seems to be necessary to consider corrections to these approximations if quantitative agreement is to be obtained at 142 MeV.

We believe that the present calculation somewhat favors the Yale phase-shift set at all energies. This conclusion must remain tentative until the corrections mentioned are considered in detail. It is, of course, possible that all of our fits to the data are fortuitous and that careful examination of the necessary corrections will show them to be major. This seems unlikely, however, in view of the fact that we obtain qualitative description of the data over large angular ranges as well as quantitative fits at small angles. Given the reasonableness of their approximations, as demonstrated in this paper, Saperstein and Feldman have shown that such qualitative fits to the data are *not* characteristic of all $N$-$N$ phase-shift sets. The use of $N$-$\mathfrak{N}$ scattering to differentiate between $N$-$N$ phase-shift sets, while not firmly proven, seems highly plausible at the present time.

PHYSICAL REVIEW VOLUME 156, NUMBER 4 20 APRIL 1967

# Optical Potential Correlation Correction from Deuteron-Nucleus Scattering*

J. F. READING†
*Laboratory for Nuclear Science and the Physics Department, Massachusetts Institute of Technology, Cambridge, Massachusetts*

(Received 21 June 1966; revised manuscript received 7 November 1966)

To describe deuteron-nucleus scattering accurately at high energies, one has to correct the approximation that the potential which acts on the deuteron is the sum of the neutron and proton optical potentials. This correction is largely due to nuclear correlations and presents a method of determining the correction to the nucleon optical potential due to correlations. The method is applied to 650-MeV deuteron-carbon scattering. Good agreement is found between theory and experiment.

## INTRODUCTION

ONE hopes that from nucleon-nucleus scattering at high energies one can get information about the two-body force and nuclear correlations. The nucleon is scattered in intermediate two-particle states "off its energy shell" and, with a wavelength of a fraction of a fermi, the strongly interacting nucleon multiply scattered from many target nucleons provides an excellent probe for nuclear correlations.[1,2] The off-energy-shell scattering leads to a nonlocality in the Watson potential. This nonlocality, which has been shown by Mulligan[3] and Reading[4] to contribute an important part to the potential, can be shown to be directly related to the derivative of the two-body $T$ matrix for "going off the energy shell."[3,4] If this extremely important information can be extracted from the experimental data, we have the possibility of nucleon-nucleus scattering becoming an extremely important tool in the study of the two-body interaction.[4] Unfortunately, the situation is somewhat complicated by the nuclear correlations, which are expected[5] to give corrections of the order of $l/R$ to the optical potential, where $l$ is the correlation length and $R$ is the nuclear radius. In this note is presented an experimental method for determining the correction to the optical model due to correlations. While some information is necessarily obtained about the correlation function, we should perhaps emphasize that this is not a method for obtaining that function, such as, for example, the methods discussed by Srivastava or Reiner.[6] The pair correlation function enters the optical potential as part of an integrand which is integrated over all the two-body space. There are contributions to this function both from short-range correlations due to the repulsive core, and from long-range correlations due to the exclusion principle and attractive forces. The correlation function for a repulsive core oscillates as the nucleons try to form a crystalline structure, but on the whole it tends to work with the exclusion principle to keep the particles apart whilst the attractive forces

* This work is supported in part through funds provided by the U. S. Atomic Energy Commission under contract AT(30-1)-2098.

† Present address: Department of Physics, University of Washington, Seattle, Washington.

[1] J. S. Levinger, Phys. Rev. **84**, 43 (1951); J. Heidmann, Phys. Rev. **80**, 171 (1951); J. Dabrowski and J. Sawicki, Nucl. Phys. **13**, 621 (1959); J. Dabrowski, Proc. Phys. Soc. (London) **71**, 658 (1958); G. M. Shklyarevsky, Zh. Eksperim. i Teor. Fiz. **41**, 234 (1961); **41**, 451 (1961) [English transl.: Soviet Phys.—JETP **14**, 170 (1961); **14**, 324 (1961)]; Tokuo Terasawa, Nucl. Phys. **39**, 563 (1962); T. I. Kopakishrili and R. I. Jubuti, *ibid.* **44**, 34 (1963); Hidetsugu Ikegami and Takeshi Udagawa, Phys. Rev. **133**, B1388 (1964).

[2] B. W. Reisenfeld and K. N. Watson, Phys. Rev. **102**, 1151 (1956); H. A. Bethe, Ann. Phys. (N. Y.) **3**, 190 (1958); A. K. Kerman, H. McManus, and R. M. Thaler, *ibid.* **8**, 551 (1959).

[3] B. Mulligan, Ann. Phys. (N. Y.) **26**, 159 (1964).

[4] J. F. Reading, Phys. Letters **20**, 518 (1966); J. F. Reading, following paper, Phys. Rev. **156**, 1116 (1967).

[5] R. Glauber, *Lectures in Theoretical Physics* (Interscience Publishers, Inc., New York, 1958), Vol. 1.

[6] Y. N. Srivastava, Bull. Am. Phys. Soc. **9**, 15 (1964); A. Reiner (private communication).